Atomic Dynamics in Liquids with Competing Interactions

Sandro Jahn* and Jens-Boie Suck

Institute of Physics, Materials Research and Liquids, TU Chemnitz, 09107 Chemnitz, Germany

(Received 18 December 2003; published 5 May 2004)

The influence of the *type* of atomic interaction on the atomic dynamics is studied for liquid Na_xSn_{1-x} ($x = 0.9, 0.77, 0.57, 0.5, 0.33$) alloys by cold neutron inelastic scattering. The dispersions obtained from the longitudinal current correlation function $J_l(Q, \omega)$ show clear evidence for the dependence of the dynamics on the type of interaction (metallic, ionic, partly covalent) tuned by changing the composition of the alloy. For the first time, a second dispersion branch is observed in the total $J_l(Q, \omega)$ around Q_p, the position of the principal peak of $S(Q)$, for the Sn-rich compositions. The dynamic properties are discussed and compared to results of recent *ab initio* molecular dynamics simulations.

DOI: 10.1103/PhysRevLett.92.185507 PACS numbers: 61.25.Mv, 61.20.Lc, 63.50.+x

The microscopic dynamics of liquids is basically understood in two limiting cases, the hydrodynamic regime, in which the system is described by continuum theory, and the region of large momentum transfers Q, where kinetic theory applies. In the intermediate region, with characteristic length scales of atomic distances and time scales of atomic interactions, the dynamics is determined by the interatomic potential and the structural arrangements of the atoms become important [1,2]. A theoretical description of this region is much more complicated due to the presence and coupling of many different dynamical processes.

Experimentally, the atomic dynamics in liquids is studied by measuring the dynamic structure factor $S(Q, \omega)$, which describes the microscopic density fluctuations, using inelastic neutron or x-ray scattering. While $S(Q, \omega)$ is dominated by contributions from free particle motions at large Q, the dynamics is very sensitive to the interatomic potential in the small Q range up to Q_p, the position of the principal peak of the static structure factor $S(Q)$ [3]. Thus far, most studies were focused on liquids with a dominant type of atomic interaction, such as liquid metals [4,5], ionic liquids [6,7], molecular liquids [8], or liquid semimetals [9]. The experiments have shown the persistence of propagating sound modes well into the nonhydrodynamic region, especially in liquid alkali metals, which may be described by generalized hydrodynamic models based on the memory function formalism [10].

The problem of how the type of atomic interaction influences the atomic dynamics was first studied in the past on liquid-metal–molten-salt mixtures [11]. These experiments revealed interesting deviations from the dynamic behavior known from simple liquids, such as an unusual shape of the dispersion relations $\omega(Q)$. However, the interpretation of the results has proven very difficult. At that time, molecular dynamics (MD) simulations using simple pair potentials were not able to reproduce the experimental data. Recent advances in electronic structure calculations and the hugely increased computing power now allow *ab initio* MD simulations, also of more complex liquids, and thus provide a means of modeling of these complicated processes with a new quality.

Especially interesting in this respect are binary systems with partly covalent bonds, e.g., intermetallic alloys of the Zintl type, made of an alkali metal and a post-transition group (semi)metal. In these alloys, the type of interaction may be tuned continuously by a change of the alloy composition. Zintl alloys show unusual thermodynamic, structural, and electronic properties [12], also in the liquid state [13]. The change in bonding is explained by a charge transfer from the alkali metal to the much more electronegative post-transition group element. Depending on the concentration, the type of bonding is changed from metallic to ionic and partly covalent. Experimental studies of the atomic dynamics in Zintl-type alloys are still rare [14], and only for liquid Rb_xSb_{1-x} alloys has a first systematic study of the concentration dependence been made [15,16].

Here we present results of inelastic neutron scattering experiments for different compositions of liquid Na_xSn_{1-x} ($x = 0.9$, 0.77, 0.57, 0.5 and 0.33). Some of the unusual properties of this alloy system have been studied experimentally as well as with *ab initio* computer simulations. The electrical resistivity has two distinct maxima, one at $x = 0.77$, near the octet composition, and the other at $x = 0.57$, close to the equiatomic composition [17]. A two-stage melting process is observed for the equiatomic alloy [18]. A prepeak as a signature of medium-ranged order in the liquid is found in the composition range between $x = 0.8$ and $x = 0.5$ in the total static structure factor $S(Q)$ [19]. From computer simulations, it is concluded that dynamic networks of polyanions exist in the liquid, and the prepeak is ascribed to a characteristic correlation length between the anions [20,21]. Furthermore, the power spectra of the velocity autocorrelation functions, which yield characteristic frequencies of the two elements in the alloy, are known from the simulations [21].

The experiments were performed on the cold neutron time-of-flight spectrometer IN6 at the High Flux Reactor

of the Institut Laue-Langevin in Grenoble. With this type of spectrometer, the Q–ω region around the principal peak Q_p of $S(Q)$ is accessed with a quasielastic resolution of 0.17 meV FWHM. We use an incident neutron energy of 4.75 meV and scattering angles between 10° and 113° are measured. The samples, prepared from the pure elements (Na: 99.95%, Sn: 99.999% purity), are contained in electron beam welded Nb cylinders with a wall thickness of 0.2 mm. The data treatment includes the corrections for the self-absorption of the sample and for multiple scattering, the latter calculated with the MSCAT code [22] from a model of $S(Q, \omega)$, which is fitted iteratively to the experimental data and extrapolated to obtain the required dynamic range (details can be found in Ref. [16]). Finally, the corrected spectra measured at constant scattering angle θ are transformed into $S(Q, \omega)$ by cubic spline fits.

The resulting total $S(Q, \omega)$ are composed of five partial contributions weighted with the respective concentrations and neutron scattering lengths:

$$\frac{\sigma_s}{4\pi} S(Q, \omega) = \sum_{i,j} \sqrt{c_i c_j}\, b_c^i b_c^j S^{ij}(Q, \omega) + \sum_i c_i \frac{\sigma_{inc}^i}{4\pi} S_s^i(Q, \omega), \quad (1)$$

with $\sigma_s = \sum_i c_i (4\pi b_c^{i2} + \sigma_{\mathrm{inc}}^i)$. c_i, b_c^i, and σ_{inc}^i are the concentration, the coherent neutron scattering length, and the incoherent neutron scattering cross section of element i, respectively. The three partial (Ashcroft-Langreth) dynamic structure factors $S^{ij}(Q, \omega)$ ($i, j =$ Na, Sn) describe the collective dynamics of the system, whereas the two self-terms $S_s^i(Q, \omega)$ ($i =$ Na, Sn) account for the single particle dynamics of the two species. For Na_xSn_{1-x} only the weighting factor of $S_s^{\mathrm{Sn}}(Q, \omega)$ is negligibly small at all concentrations. The other contributions are present in the measured spectra with changing weight. However, since the weighting factors change *monotonously* with concentration, any discontinuous behavior of the dynamic properties can be attributed to actual changes of the dynamics in the system due to the different types of interaction.

Integrating $S(Q, \omega)$ over ω yields the zeroth frequency moment of the dynamic structure factor, the total $S(Q)$ [16], which is in good agreement with $S(Q)$ obtained from diffraction experiments [17]. The most prominent changes in $S(Q)$ as a function of concentration are the shift of the principal peak position Q_p with composition and the appearance of the prepeak between $x = 0.8$ and $x = 0.5$.

The spectral shape of the dynamic structure factor of liquids is often interpreted by fitting models of different complexity to cuts of $S(Q, \omega)$ at constant Q. However, theoretical descriptions of binary systems beyond the hydrodynamic regime are still not fully developed but necessarily involve a large number of parameters. Therefore, ambiguous approximations have to be made if the fit of a model to experimental data is attempted. Models such as the damped harmonic oscillator (fitted together with a Lorentzian to describe the quasielastic peak) or the more advanced generalized hydrodynamic model for monatomic liquids (as, e.g., employed in [5]) here fail to fit the $S(Q, \omega)$ systematically in the Q range of IN6 and for the different samples. On the other hand, the generalization of a viscoelastic model to binary systems [23] exists, but due to the large number of parameters it is not suited for an experimental fitting procedure.

An alternative approach to discuss the dynamic structure on a qualitative level makes use of a simple relationship between $S(Q, \omega)$, the correlation function of the particle densities, and $J_l(Q, \omega)$, the correlation function of the longitudinal currents:

$$J_l(Q, \omega) = \frac{\omega^2}{Q^2} S(Q, \omega). \quad (2)$$

Cuts through $J_l(Q, \omega)$ at two constant Qs for the different concentrations are shown in Fig. 1. At each Q, $J_l(Q, \omega)$ exhibits at least one peak at finite energy transfers ω_m, which vary with Q and concentration. Beside the broad maximum present in all spectra of Fig. 1, a second sharper peak appears at small energy transfers for the Sn-rich concentrations. For the sample with 33 at. % Na, this second peak even becomes dominant around the principal maximum of $S(Q)$, i.e., around $Q_p = 23\ \mathrm{nm}^{-1}$ at this composition. Given that the second dispersion branch is observed only in the spectra of the Sn-rich alloys, it is plausible to attribute it to the motions of the Sn atoms. There is indeed strong evidence for this assignment as will be discussed below.

When the maxima of $J_l(Q, \omega)$ are plotted as a function of Q, a dispersion relation $\omega_m(Q)$ is obtained [see Fig. 2(a)]. The dispersion curves describe the evolution of dynamic modes using the longitudinal currents rather than density fluctuations as dynamic variables. In the present experiment, the dynamic range around Q_p is measured. Close to Q_p, the spectral functions (of any liquid) are considerably narrowed and the dynamics of the time correlation function slows down, which leads to a minimum in the dispersion relation. Hence, the position of the minimum of ω_m in Q should follow closely the shift of Q_p in $S(Q)$. This behavior of ω_m is indeed observed. Starting from the alkali-rich side, the minimum of the high frequency dispersion in Fig. 2(a) first shifts towards larger Q, up to about $x = 0.5$, where the covalent effects are expected to be strongest. Beyond the equiatomic composition the trend is reversed, in agreement with $S(Q)$ [16]. In the covalent regime the bonds are expected to be strongest leading to the smallest interatomic separations. Smaller characteristic distances translate into larger Q in reciprocal space.

The shift of the minimum is not restricted to the Q scale. When the interaction between the atoms becomes stronger, the dispersion is also shifted to higher frequencies. It is again for the equiatomic alloy that the minimum of ω_m reaches its maximum value, now in the

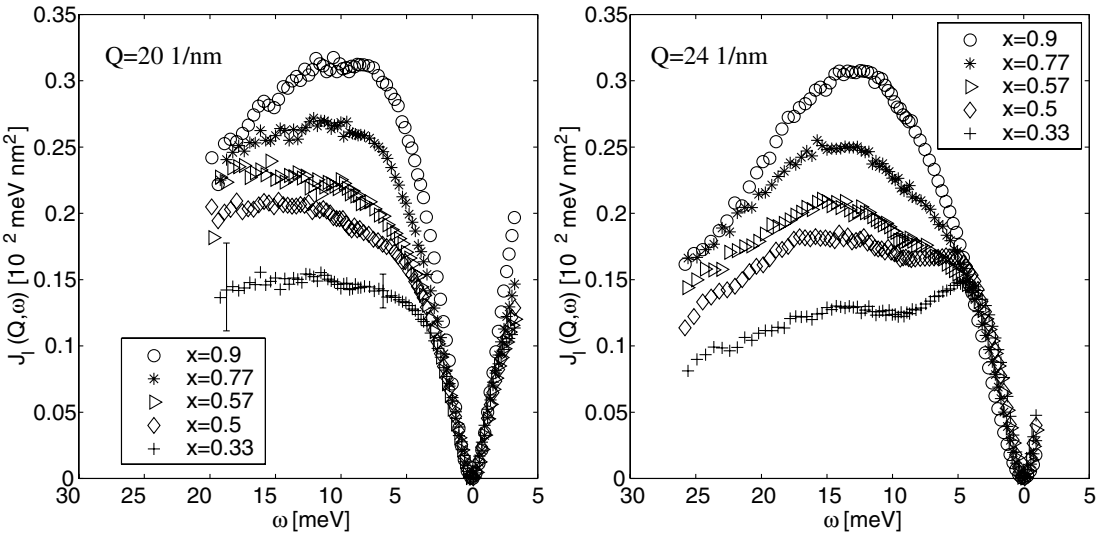

FIG. 1. $J_l(Q, \omega)$ of liquid Na_xSn_{1-x} alloys for different concentrations and momentum transfers Q, still convoluted with the resolution function. At $Q = 24$ nm^{-1}, a second, low frequency branch is growing with increasing Sn concentration. The error bars decrease considerably towards low energy transfers since the measured $S(Q, \omega)$ has its maximum at $\omega = 0$.

frequency domain. The shift of the dispersion towards smaller ω between $x = 0.5$ and $x = 0.33$ is confirmed in the lower dispersion branch.

The observation of two dispersion branches is quite spectacular since it allows an at least qualitative discussion of the different dynamic behavior of the two components of the alloy without having access to the partials, $J_l^{ij}(Q, \omega) = \omega^2/Q^2 S^{ij}(Q, \omega)$. Besides the aforementioned argument regarding the concentrations, there is further strong evidence for the assignment of the lower branch to the dynamics of the Sn atoms, whereas the high frequency branch should mainly stem from the Na atoms.

Even if, due to the influence of the potential, the dynamics of the two elements is likely to be different in detail, the spectra of the vibrational frequencies should roughly scale with the inverse ratio of the square roots of the atomic mass M. Here the expected scaling ratio,

$$\omega_{\mathrm{Na}}/\omega_{\mathrm{Sn}} \sim \sqrt{M_{\mathrm{Sn}}/M_{\mathrm{Na}}} \sim 2.3, \tag{3}$$

is almost fulfilled when the frequencies of the minima of ω_m are considered. For $x = 0.5$, a quantitative comparison to results of *ab initio* computer simulations [21] can be made. In these simulations the Fourier transforms of the velocity autocorrelation functions were calculated. The resulting power spectra $z^i(\omega)$ (i = Na, Sn) would correspond in a harmonic crystal to the vibrational density of states for one-phonon processes.

The maxima of $z^{\mathrm{Na}}(\omega)$ and $z^{\mathrm{Sn}}(\omega)$ derived from the simulations are found at 17 and 5 meV, respectively [see Fig. 2(b)]. The agreement with the minima of ω_m (14 and 6 meV) is remarkably good, bearing in mind that these characteristic frequencies are derived from different correlation functions. Another similarity between the experiment and the simulation is related to the widths of the spectra. As shown in Fig. 1, the peak in $J_l(Q, \omega)$ related to the Sn atoms is much sharper than the other one. The same tendency is observed in the $z^i(\omega)$, where $z^{\mathrm{Na}}(\omega)$ is in fact very broad. We have attempted to extract an approximate of the total $z(\omega)$ [a weighted superposition of $z^{\mathrm{Na}}(\omega)$ and $z^{\mathrm{Sn}}(\omega)$] from the experimental data by generalizing the relation [24]

$$z(\omega) = \lim_{Q \to 0} \frac{\omega^2}{Q^2} S_s(Q, \omega) \tag{4}$$

to the measured total $S(Q, \omega)$. For sufficiently large energy transfers, the coherence effects in $S(Q, \omega)$ are small

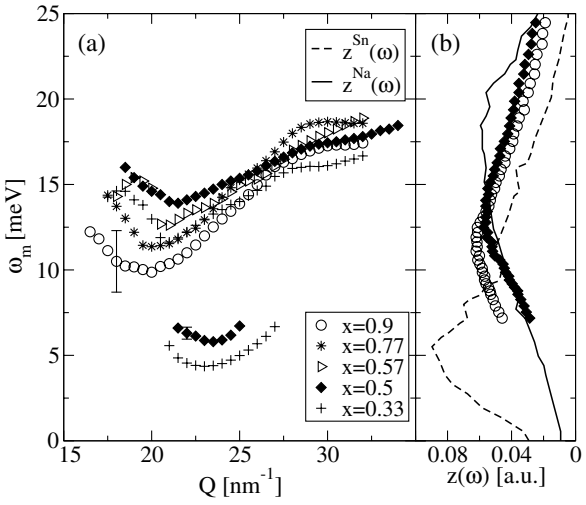

FIG. 2. (a) Dispersions from the maxima of $J_l(Q, \omega)$ at $T = 820$ K (930 K for $x = 0.5$, which has negligible influence on ω_m [16]). Typical error bars are indicated in two cases. (b) Total vibrational frequency spectra $z(\omega)$ for two concentrations obtained using the extrapolation scheme described in the text (symbols) and partial $z^i(\omega)$ from *ab initio* MD simulations (lines) from Ref. [21].

enough to allow a sensible averaging of $\omega^2/Q^2 S(Q, \omega)$ over the measured Q range at constant ω values with a linear regression and an extrapolation of the regression line to $Q = 0$ [16,25]. Each total $z(\omega)$ shows one peak that is found between $\omega = 11$ and 13 meV, the shift of its position resembling the behavior of the dispersion ω_l (see Fig. 2). For $x = 0.5$, the maximum is found at 13 meV, which compares well with the *ab initio* value of 12 meV of the respective $z(\omega)$ [weighted superposition of the *ab initio* $z^i(\omega)$]. However, with the extrapolation procedure it is not possible to reproduce the sharp peak of the $z^{\mathrm{Sn}}(\omega)$ contribution expected at about 5 meV, since the coherence effects are too strong close to the quasielastic line.

A splitting of the dispersion ω_m has also been observed and discussed in a theoretical study of a binary mixture of simple liquids using a viscoelastic model for two-component systems [23]. As in the present case, the low energy dispersion branch is visible only around Q_p, where due to the *de Gennes* narrowing [26] the diffusive modes contribute much less to the total $J_l(Q, \omega)$, while it is hidden by the broad quasielastic line outside this Q region. The two maxima of $J_l(Q, \omega)$ are assigned to two propagating modes: one at low frequency that resembles an acoustic mode and accounts for the slow in-phase motion of the heavy atoms, and the other described as a high frequency optic mode where the light atoms move out of phase with the heavy atoms. Hence, at small Q (not accessible in the present experiment) the high frequency mode should tend to a nonvanishing energy, whereas the slow mode would eventually merge in the linear hydrodynamic dispersion. While the two dispersion branches for the mixture of simple liquids have their minimum at the same Q value [23], the covalent bonds between Sn atoms in the Na_xSn_{1-x} alloys seem to cause a shift of the dispersion minimum of the low energy dispersion towards larger Q. This is again consistent with chemical picture, i.e., a stronger (and, hence, shorter) bond between the Sn atoms compared to the bonds between the Na atoms. The interpretation of the origin of the two modes is consistent with and clarifies findings from a neutron study on liquid Li_4Pb alloys [7].

We wish to acknowledge the allocation of beam time by the ILL Grenoble, and thank M. Koza and S. Jenkins for their support during the start-up of the experiment, and H. Teichmann for the sample preparation. This work was supported by DFG Grant No. SU 176/10-1.

*Present address: Physical and Theoretical Chemistry Laboratory, University of Oxford, Oxford OX1 3QZ, United Kingdom.
Electronic address: sandro.jahn@chem.ox.ac.uk

[1] J. P. Boon and S. Yip, *Molecular Hydrodynamics* (McGraw-Hill, New York, 1980).
[2] U. Balucani and M. Zoppi, *Dynamics of the Liquid State* (Oxford University Press, New York, 1994).
[3] G. Pratesi, J.-B. Suck, and P. A. Egelstaff, J. Non-Cryst. Solids **250–252**, 91 (1999).
[4] J. R. D. Copley and J. M. Rowe, Phys. Rev. Lett. **32**, 49 (1974); L. E. Bove, F. Sacchetti, C. Petrillo, B. Dorner, F. Formisano, and F. Barocchi, Phys. Rev. Lett. **87**, 215504 (2001).
[5] T. Scopigno, U. Balucani, G. Ruocco, and F. Sette, Phys. Rev. Lett. **85**, 4076 (2000).
[6] R. L. McGreevy, E. W. J. Mitchell, F. M. A. Margaca, and M. A. Howe, J. Phys. C **18**, 5235 (1985); H. Sinn, B. Glorieux, L. Hennet, A. Alatas, M. Hu, E. E. Alp, F. J. Bermejo, D. L. Price, and M.-L. Saboungi, Science **299**, 2047 (2003).
[7] M. Alvarez, F. J. Bermejo, P. Verkerk, and B. Roessli, Phys. Rev. Lett. **80**, 2141 (1998).
[8] U. Bafile, P. Verkerk, F. Barocchi, L. A. de Graaf, J.-B. Suck, and H. Mutka, Phys. Rev. Lett. **65**, 2394 (1990); U. Bafile, P. Verkerk, E. Guarini, and F. Barocchi, Phys. Rev. Lett. **86**, 1019 (2001).
[9] S. Hosokawa, Y. Kawakita, W.-C. Pilgrim, and H. Sinn, Phys. Rev. B **63**, 134205 (2001); T. Scopigno, A. Filipponi, M. Krisch, G. Monaco, G. Ruocco, and F. Sette, Phys. Rev. Lett. **89**, 255506 (2002).
[10] H. Mori, Prog. Theor. Phys. **33**, 423 (1965).
[11] C. Mathieu, J.-F. Jal, J. Dupuy, J.-B. Suck, and P. Chieux, Nuovo Cimento **12D**, 673 (1990); P. Chieux, J. Dupuy-Philon, J.-F. Jal, C. Morkel, and J.-B. Suck, J. Phys. Condens. Matter **6**, A235 (1994).
[12] *Chemistry, Structure and Bonding of Zintl Phases and Ions*, edited by S. M. Kauzlarich (VCH Publishers, New York, 1996).
[13] W. van der Lugt, J. Phys. Condens. Matter **8**, 6115 (1996).
[14] H. T. J. Reijers, M.-L. Saboungi, D. L. Price, J. W. Richardson, K. J. Volin, and W. van der Lugt, Phys. Rev. B **40**, 6018 (1989); D. L. Price, M.-L. Saboungi, and W. S. Howells, Phys. Rev. B **51**, 14 923 (1995).
[15] S. Jahn, G. Pratesi, and J.-B. Suck, Appl. Phys. A **74**, S1664 (2002).
[16] S. Jahn, Ph.D. thesis, TU Chemnitz, 2003.
[17] C. van der Marel, A. B. van Oosten, W. Geertsma, and W. van der Lugt, J. Phys. F **12**, 2349 (1982).
[18] M.-L. Saboungi, J. Fortner, W. S. Howells, and D. L. Price, Nature (London) **365**, 237 (1993).
[19] B. P. Alblas, W. van der Lugt, J. Dijkstra, W. Geertsma, and C. van Dijk, J. Phys. F **13**, 2465 (1983); M. Stolz, O. Leichtweiß, R. Winter, M.-L. Saboungi, J. Fortner, and W. S. Howells, Europhys. Lett. **27**, 221 (1994).
[20] G. Seifert, R. Kaschner, M. Schöne, and G. Pastore, J. Phys. Condens. Matter **10**, 1175 (1998).
[21] O. Genser and J. Hafner, J. Phys. Condens. Matter **13**, 981 (2001).
[22] J. R. D. Copley, P. Verkerk, A. A. Van Well, and H. Frederikze, Comput. Phys. Commun. **40**, 337 (1986).
[23] Y. Chushak, T. Bryk, A. Baumkertner, G. Kahl, and J. Hafner, Phys. Chem. Liq. **32**, 87 (1996).
[24] P. A. Egelstaff and P. Schofield, Nucl. Sci. Eng. **12**, 260 (1962).
[25] S. Jahn and J.-B. Suck, J. Non-Cryst. Solids **312–314**, 134 (2002).
[26] P. G. de Gennes, Physica (Utrecht) **25**, 825 (1959).